

Cite this: *Lab Chip*, 2015, 15, 563

Fine structuration of low-temperature co-fired ceramic (LTCC) microreactors†

Bo Jiang,^{*ab} Julien Haber,^c Albert Renken,^c Paul Muralt,^a Lioubov Kiwi-Minsker^c and Thomas Maeder^{*b}

The development of microreactors that operate under harsh conditions is always of great interest for many applications. Here we present a microfabrication process based on low-temperature co-fired ceramic (LTCC) technology for producing microreactors which are able to perform chemical processes at elevated temperature ($>400\text{ }^{\circ}\text{C}$) and against concentrated harsh chemicals such as sodium hydroxide, sulfuric acid and hydrochloric acid. Various micro-scale cavities and/or fluidic channels were successfully fabricated in these microreactors using a set of combined and optimized LTCC manufacturing processes. Among them, it has been found that laser micromachining and multi-step low-pressure lamination are particularly critical to the fabrication and quality of these microreactors. Demonstration of LTCC microreactors with various embedded fluidic structures is illustrated with a number of examples, including micro-mixers for studies of exothermic reactions, multiple-injection microreactors for ionone production, and high-temperature microreactors for portable hydrogen generation.

Received 19th September 2014,
Accepted 11th November 2014

DOI: 10.1039/c4lc01105h

www.rsc.org/loc

Introduction

Chemical microreactors are a type of meso-scaled reaction systems that have fluidic channels with characteristic dimensions in the sub-millimeter range. By combining process intensification concepts with microfabrication techniques, these microreactors have been rapidly developed to perform liquid/gas phase chemical reactions, particularly the quasi-instantaneous endothermic or exothermic ones.^{1,2} Ceramic materials in general feature high chemical and thermal stability. Hence they are very preferable to be used as reactor construction materials, especially for reactors involved with high temperature and/or harsh chemical reactions.^{3–10} Knitter *et al.*³ have demonstrated alumina-based reactors using an injection molding process, in which the molds were fabricated through a stereolithography method. These reactors contain various micro-scale fluidic structures and can be applied up to $1100\text{ }^{\circ}\text{C}$. Meschke and his team⁵ have developed a microchannel fabrication process based on laser machining or milling for producing silicon carbide (SiC) reactors. Compared to alumina and SiC, in terms of material properties, fired LTCC devices have a relatively low operating temperature that is feasible for any process below $800\text{ }^{\circ}\text{C}$

(ref. 11) and they show good resistance to certain kinds of aggressive wet chemicals.¹² More importantly, the LTCC technology – a multiple layer based manufacturing method – exhibits several advantages over other ceramic fabrication processes. LTCC is very compatible with thick film technology: they have very similar peak processing temperatures, usually in the range of $850\text{--}900\text{ }^{\circ}\text{C}$, and thick film conductive or resistive materials can either be screen printed on LTCC green tapes and fired together in a one-step manufacturing process (“co-fired”) or directly fabricated on fired LTCC (“post-fired”).¹³ It consequently promotes the integration ability of electronic components, such as sensors, actuators and electrical packaging, in LTCC devices for realizing accurate process control and real-time automation.^{14,15} Another advantage of LTCC for making microreactors is that their green tapes appear flexible and can be easily machined to create cavities *via* milling,¹⁶ embossing,¹⁷ laser cutting,¹⁸ and use of sacrificial materials.¹⁹ Through stacking and laminating these green tapes with cavities in 3D, these stacks can incorporate various embedded or open fluidic structures in the sub-mm scale, such as packed beds,²⁰ microchannels,⁹ heat exchangers²¹ and mixers, for desired chemical processes.²² Besides, LTCC technology is a low-cost manufacturing method and requires less investment and maintenance cost than silicon-based microfabrication ones, making it suitable for both high-volume production and fast prototyping cycles.

The incorporation of fluidic structures into LTCC microreactors primarily depends on the lamination process. Standard ones (isostatic or uniaxial thermocompression) cannot

^a Ceramics Laboratory, EPFL, Lausanne, Switzerland. E-mail: bo.jiang@alumni.epfl.ch

^b Laboratory of Microengineering for Manufacturing, EPFL, Lausanne, Switzerland. E-mail: thomas.maeder@epfl.ch

^c Group of Catalytic Reaction Engineering, EPFL, Lausanne, Switzerland

† Electronic supplementary information (ESI) available. See DOI: 10.1039/c4lc01105h

be used as the embedded fluidic structures (*e.g.* channels or cavities) get easily damaged in the stacked LTCC tapes by the high lamination temperature and/or pressure, causing sagging, tearing and cracking issues. Several approaches have been proposed so far in order to reduce these deformations and improve the quality of integrated LTCC fluidic structures. One method is using temporary inserts to introduce mechanical supports to the LTCC cavities to avoid deformation and/or sagging during lamination. These inserts, usually solid flexible objects,²³ are removed right after lamination. However, the removal of inserts from the laminate can cause permanent damage to these fluidic structures. Besides, this method is not applicable for fabricating fully embedded fluidic channels.

Alternatively, a chemical-assisted lamination process has been proposed that enables low-pressure and/or low-temperature bonding of LTCC green tapes. Roosen *et al.*²⁴ used double-sided adhesive tape that contains acrylate adhesives and a polyethylene terephthalate (PET) film to ensure temporary binding of green tapes under a low lamination pressure at ambient temperature. Upon heating (40–60 °C), these adhesives, together with the binders in the LTCC green tapes, soften and join the laminates through capillary forces. Aside from adhesives, chemical solvents are also used for temporary gluing of LTCC green tapes at low pressure and room temperature.^{18,25} These solvents are usually some of the organic compositions of LTCC green tapes or thick film materials. Although these methods are proven to achieve sustainable LTCC cavities with very minimal deformation, their process reliability can be a potential issue in integrating thick film materials or electrical vias. On the other hand, these binding agents introduce additional organic contents into LTCC laminates and exacerbate their debinding process during firing,²⁶ which eventually increases the manufacturing lead time and cost.

Another solution is to use sacrificial volume materials (SVM). These SVMs are placed into the stacked LTCC tapes to provide mechanical support as well as prevent the embedded fluidic channels from collapsing and/or deforming during the lamination and/or firing process. Common SVMs are carbon-based fugitive materials^{27,28} which generally burn out from LTCC samples between the debinding and sintering stages. Organic SVMs such as waxes and polymers^{18,29} are also used which burn out only during the debinding step. The drawback of using SVMs is the extended firing time, increasing manufacturing costs greatly. Moreover the residual SVMs in the fluidic channels, which are left in the device due to an incomplete burn out process, can contaminate the reactions carried out and/or the installed catalyst, hindering the microreactor's performance.

The reference review above has clearly shown the current limitations of fabricating embedded fluidic structures in LTCC-based microreactors. To overcome these issues, we present a simple and reliable microfabrication strategy for developing LTCC-based microreactors with integrated fine and complex fluidic structures. The proposed process is a combination of laser micromachining, multi-step lamination,

and a firing process. In order to produce LTCC microreactors with intact fluidic structures, various optimization studies of these processes have been carried out in this work. The optimized microfabrication not only enabled us to incorporate complex fluidic structures into the microreactors but also granted us wide opportunities to develop LTCC microreactors for applications of harsh chemical processes. Using our developed microfabrication process, several novel LTCC microreactors in the range of mm to sub-mm are demonstrated here, including micro-mixers for studying chemical reactions with fast intrinsic kinetics and high exothermicity; multi-injection microreactors for ionone production; and multi-functional high-temperature microreactors for on-site hydrogen production.

Experimental

Stability test

In order to perform reactions of harsh chemicals, the LTCC's material stability must be qualified first. To do so, fired LTCC samples were observed in terms of their etching behavior in several kinds of chemically aggressive aqueous solutions. The LTCC materials used were 951 Green Tape™ (DP951, DuPont USA) and HeraLock® 2000 (HL2K, Heraeus Germany). DP951 is a conventional LTCC material made of calcium aluminosilicate glass and alumina fillers that has a planar shrinkage of 12.7% (*X*- and *Y*-axes) after firing.³⁰ HL2K, on the other hand, has a more complex three-layer structure, in which the refractory ceramic layer is sandwiched between outer layers rich in glass phase. Upon firing, these layers constrain mutually resulting in HL2K having a nearly zero fired planar shrinkage.³¹ For the material stability evaluation, 3 pieces of LTCC green tapes for each kind were cut into sizes of 10 × 20 mm², laminated and fired under standard manufacturing conditions.^{32,33} The thickness of the fired DP951 and HL2K samples was 0.29 mm and 0.27 mm, respectively. Standard alumina pieces (grade 96%, thickness: 1.0 mm, Haldemann & Porret SA, Switzerland) with similar sizes were used in the test as references. The tested chemicals included 2.0 mol L⁻¹ sodium hydroxide (NaOH), 9.1 mol L⁻¹ sulfuric acid in water (H₂SO₄) and 0.2 mol L⁻¹ hydrochloric acid in water (HCl). These wet chemicals with defined concentrations are commonly used in industrial chemical reactions.² The concentrated sodium hydroxide solution was additionally used to investigate the leaching stability of the LTCC materials, as the silicate-based glass content of LTCC is very soluble in this condition.¹³ The weight loss of LTCC and alumina samples, stored at room temperature, was measured after 1, 2 and 4 weeks. The chemical stability of all tested samples was compared in terms of the cumulative weight loss (ΔW), normalized by the surface area of the tested samples as defined in eqn (1).

$$\Delta W = \frac{W_0 - W_x}{S}, (x = 1, 2, 4) \quad (1)$$

Laser micromachining of LTCC fluidic structures

Laser micromachining is widely considered as one of the most versatile methods for structuring fluidic cavities in individual LTCC green tapes, at least for prototypes or small series production. This is mainly because of its fine structure resolution, the absence of mechanical contact with the tape surface for minimal contamination, and high processing speed. In this work, the laser structuration was carried out using a diode pumped Nd:YAG trimming laser source (LS9000, wavelength: 1064 nm, power output: 3 W, spot size: 50 μm , Laser Systems, Germany) equipped with a computer-controlled galvanometric beam deflection system. The laser beam with a wavelength of 1064 nm has been generally identified to be suitable for machining LTCC green tapes.^{34,35} A herringbone structure served for this study. The structure contained several parallel groove frameworks (100 μm wide) in a 500 μm wide fluidic channel. The dependence of the machining quality in the LTCC green tapes on the diode power, I [W]; the frequency of the optical switch, f [kHz]; and the velocity of the deflected beam, v [mm s^{-1}] was evaluated. The quality of the machined test structures in both HL2K (tape thickness: 133 μm) and DP951 (tape thickness: 245 μm) green tapes was examined by optical microscopy (M165C, Leica Microsystems Inc., Germany).

Multi-step lamination process

In order to fabricate complex embedded fluidic structures with little damage in LTCC devices, we propose a modified uniaxial lamination process. Fig. 1 shows a schematic of our approach, which basically consists of pre-lamination at standard lamination pressure and room temperature, and low-pressure lamination at elevated temperature. For the pre-lamination, since all LTCC tapes in the sub-laminates have identical cavities, the standard lamination pressure can be applied without concerns of damaging the fluidic structures. Such a step aims (i) to increase the height of the cavities to obtain the desired aspect ratio of the fluidic

channels; (ii) to increase the overall thickness of the sub-laminates for enhanced mechanical strength during low-pressure lamination; and (iii) to avoid delamination in the stacks where some multiple layers of LTCC tapes are sandwiched between cavities and receive no lamination pressure on both sides.

The second lamination process, although only one step is shown in Fig. 1 and used for the test, can be made for several stages for the cases with complex fluidic structures. It is expected that the organic binder content of the tapes becomes soft at elevated temperature to join the stacked sub-laminates suitably only at a relatively low compressive pressure. In such a way, the deformation or collapse of the embedded LTCC fluidic structures can be prevented, while good joining of the stacks is still achievable. It is primarily the increased thickness of the sub-laminates which improves their mechanical strength and minimizes their deformation during the low-pressure lamination. This method is especially effective in situations wherein some multiple layers sub-laminates are sandwiched between cavities from other sub-laminates and receive no pressing force during joining.

A similar approach has been mentioned in previous work;³⁶ however, there are no details available with regard to the lamination process. Specifically the optimized lamination processing parameters and their influence on LTCC material variants and fluidic structure complexity are unknown. Besides, the feasibility of using such a method in developing LTCC microreactors is still an open question to us. Thus, for the first time, we conducted a more quantitative and comprehensive investigation into the optimization of low-pressure lamination of DP951 and HL2K materials.

The optimization study mainly focused on the second step, the low-pressure lamination. A test sample was designed for evaluating the influence of T and P on the deformation of the embedded fluidic channels. As shown in Fig. 2a, a cavity was cut in the DP951 (tape thickness: 245 μm) or HL2K (tape thickness: 133 μm) green tapes by laser micromachining having a length of 10 mm and a

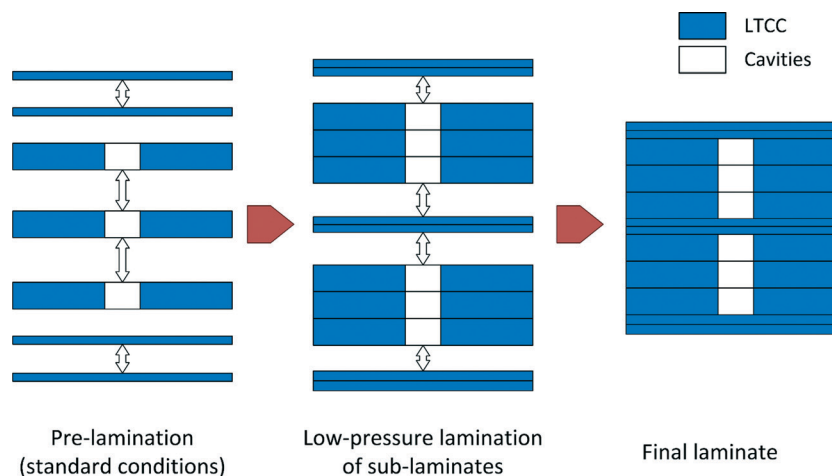


Fig. 1 A schematic view of the multi-step lamination process.

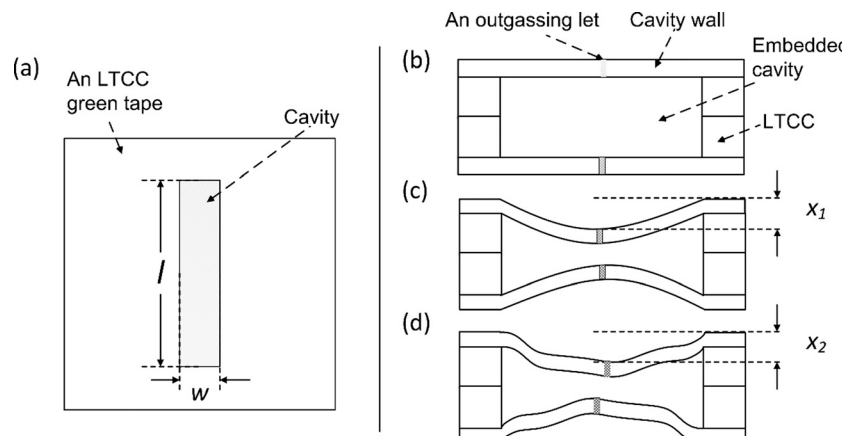


Fig. 2 Schematic views of the multi-step lamination optimization test: (a) a LTCC green tape with a test cavity; (b) the cross section of laminates with embedded cavities before lamination; (c) the deflection in the samples after the lamination; and (d) the deflection in the samples after the firing.

varying width (w), from 0.2 to 1.2 mm. For each kind of LTCC material, three pieces of tapes with the same cavities were first laminated at lamination pressure $P = 20$ MPa and lamination temperature $T = 25$ °C. These sub-laminates were then stacked with two blank tapes to embed the cavities (see Fig. 2b), on which two outgassing outlets were made with a diameter of 0.2 mm. Low-pressure lamination was then performed on these stacks by various combinations of $T = 40\text{--}90$ °C and $P = 2\text{--}8$ MPa. A total of 7 lamination conditions were used for the low pressure lamination (see Table 1). Three samples were fabricated under each set of test conditions. Then these prepared laminates were sintered using their standard firing process explained in Table 2.

The quality of these embedded fluidic cavities was mainly evaluated using the deflection profile of the suspended LTCC parts over the embedded cavities or, in other words, the deformation of the cavity walls, which was obtained with an optical profilometer (UBM optical profilometer, optical beam spot size: 50 nm, UBM Corporation, Germany). The maximum deflection of such walls after lamination, Δh_1 , is defined by eqn (2) (see Fig. 2c). After firing, these deflections might further develop, leading to an unpredictable profile due to LTCC shrinkage. It should be noted that the

deformations shown in Fig. 2d are only one of many possibilities and the actual deformation would be known from the profilometric results. We defined the maximum deflection after firing as Δh_2 given by eqn (3). In addition, the cross section of all test samples was evaluated by optical microscopy.

$$\Delta h_1 = x_1 \quad (2)$$

$$\Delta h_2 = x_2 - x_1 \quad (3)$$

Results and discussion

Chemical resistance of the LTCC materials

The chemical stability of alumina, DP951 and HL2K tapes was examined in NaOH, H₂SO₄ and HCl solutions by aging tests. Both alumina and DP951 remained the same in their weight and appearance in all tested solutions. Although it contains a certain amount of glass phase, DP951 exhibited a very low etching rate (<0.001 g mm⁻²) in NaOH. In contrast, HL2K showed lower resistance to NaOH with more weight loss after 4 weeks of aging (~0.064 mg mm⁻²). We believe that HL2K's tape structure and composition, especially its glass

Table 1 Process parameters for the low pressure lamination test

Lamination test	1	2	3	4	5	6	7
Temperature	70 °C	70 °C	70 °C	40 °C	60 °C	70 °C	90 °C
Pressure	2 MPa	4 MPa	8 MPa	2 MPa	2 MPa	2 MPa	2 MPa

Table 2 The firing process of the tested LTCC materials

Firing profile	DP951	HL2K
Organic burnout	25 °C to 400 °C at 13 °C min ⁻¹ 400 °C to 600 °C at 4.6 °C min ⁻¹	25 °C to 100 °C at 3 °C min ⁻¹ 100 °C to 450 °C at 2 °C min ⁻¹
Ceramic sintering	600 °C to 895 °C at 7.1 °C min ⁻¹ 30 min dwell	450 °C to 865 °C at 8 °C min ⁻¹ 30 min dwell
Cooling	895 °C to 50 °C at 20.5 °C min ⁻¹	865 °C to 50 °C at 10 °C min ⁻¹

content, certainly affected its chemical stability against the NaOH solution more seriously than that of the others.³⁷

The HL2K composition showed very weak resistance to the acidic environment, as compared with DP951. This is in agreement with previous studies tested in dilute HCl,³⁷ acetic and phosphoric acids.³⁸ Within 1 week, the HL2K samples were totally dissolved in HCl at room temperature (data not shown). In the case of H₂SO₄, the ΔW of the HL2K ones was about 0.01 mg mm⁻² after 4 weeks of aging (see Fig. 3). The generally poor acid resistance of HL2K agreed with the results in other studies.³¹ They seem to exhibit less severe degradation in H₂SO₄ than in HCl. HL2K is rich in calcium and lanthanum oxides, such as CaAl₂B₂O₇ and LaBO₃, and is not supposed to be very acid-resistant.³⁹ Therefore the formed calcium sulfates (CaSO₄) on the surface of the HL2K ones have very limited solubility in H₂SO₄ and they actually acted as a passivation layer and prevented further etching. To further verify our assumption, detailed chemical studies using energy dispersive spectroscopy on the surface of the tested HL2K samples will be conducted in the next step. Moreover, the tape structure of HL2K is believed to be another explanation for its weak acidic resistance. As Rabe *et al.*³¹ indicated, HL2K is a composite of three layers of ceramic thin tapes sandwiched together, with outer porous layers rich in glassy phase. These outer layers can easily be reacted with aggressive chemicals, resulting in fast dissolution especially in HCl, compared with DP951 that has a more homogenous structure of mixed glass and refractory materials. Overall, we conclude that DP951 appears to be more stable in the presence of aggressive aqueous chemicals, and hence more suited for microreactor applications.

Laser micromachining of LTCC green tapes

Fig. 4a depicts the herringbone structure with the designed dimensions for laser processing optimization which contains several parallel groove frameworks: 100 µm wide each in a

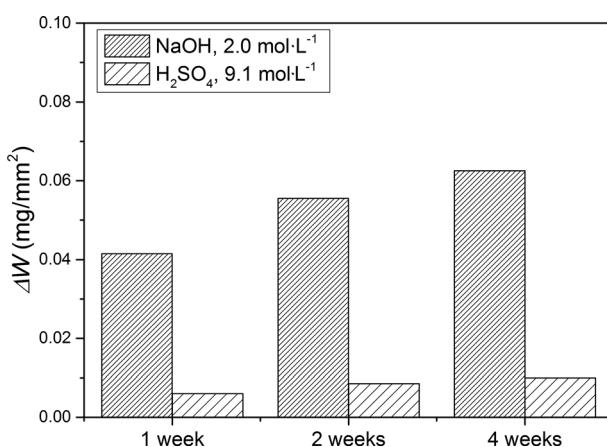


Fig. 3 Chemical stability results of fired HL2K LTCC in 2.0 mol L⁻¹ sodium hydroxide (NaOH) and 9.1 mol L⁻¹ sulfuric acid (H₂SO₄) aqueous solution.

500 µm wide fluidic channel. The dimension of such a test structure is close to the spot size of our laser beam source and reaches to the limitation of the structuration that our instrument can handle. Generally, evaluation showed that low incident energy was produced by using high *f* and *v* as well as low *I* towards the LTCC green tapes, resulting in inefficient melting or removal of the DP951 or HL2K materials. This led to incomplete cuts or partial removal of materials from the samples, as illustrated by the DP951 ones in Fig. 4d. In contrast, low *f* and *v* with high *I* generated excessive incident energy into the green tapes, resulting in rough and/or burnt edges, bulging cuts, and damaged herringbone structures (see Fig. 4e & f). By combining these parameters at optimized levels, herringbone structures of good quality were achieved in both HL2K (see Fig. 4b) and DP951 (see Fig. 4c), wherein *I* corresponded to 1.2 W and *f* and *v* were 8 kHz and 10 mm s⁻¹, respectively.

Aside from laser micromachining, it is believed that good quality structures also depend on the kinds of LTCC materials, with respect to their tape structure, absorption coefficient, and thermal conductivity. This can be seen from the comparison of cut herringbone structures between HL2K and DP951 (see Fig. 4b & c). There were more burnt and ragged edges under identical process conditions in HL2K; however it (133 µm) was slightly thicker than DP951 (113 µm). We suggest that the porous and glassy outer layers in the HL2K samples are mainly responsible for this difference, as they are melted easier by the laser compared to the DP951 ones, which have a mesoscopically homogenous mixture of glass, ceramic and organic materials.⁴⁰

Multi-step lamination process

Fig. 5 shows the maximum deflections of the embedded cavities with varying *w* in the DP951 and HL2K samples which were formed during the secondary lamination (Δh_1) and firing (Δh_2) stages under various conditions of *T* and *P*. These deformations under the same conditions generally have a deviation of ± 0.5 µm, which is mostly due to the inherent variation of the lamination process and/or errors in the profilometric measurement. Nevertheless, these results show a clear trend in both the DP951 and HL2K cases: the deflection of the embedded cavity walls developed with increasing *T*, *P* and *w*.

As seen from Fig. 5a, c, e & g, for both samples, a sunken surface on the walls of the embedded cavities after the lamination process was generally observed. The HL2K samples generally deformed more than the DP951 ones, indicating that their cavity walls have less mechanical strength against the lamination process. One may argue this is due to the thinner cavity walls that the HL2K ones have (133 µm in the green state) as compared with those of DP951 (254 µm in the green state). We then compared both samples made under identical conditions with a similar thickness of cavity walls for HL2K (266 µm) and DP951 (254 µm) in the green state. The same trend in deformation was found (see Fig. S1

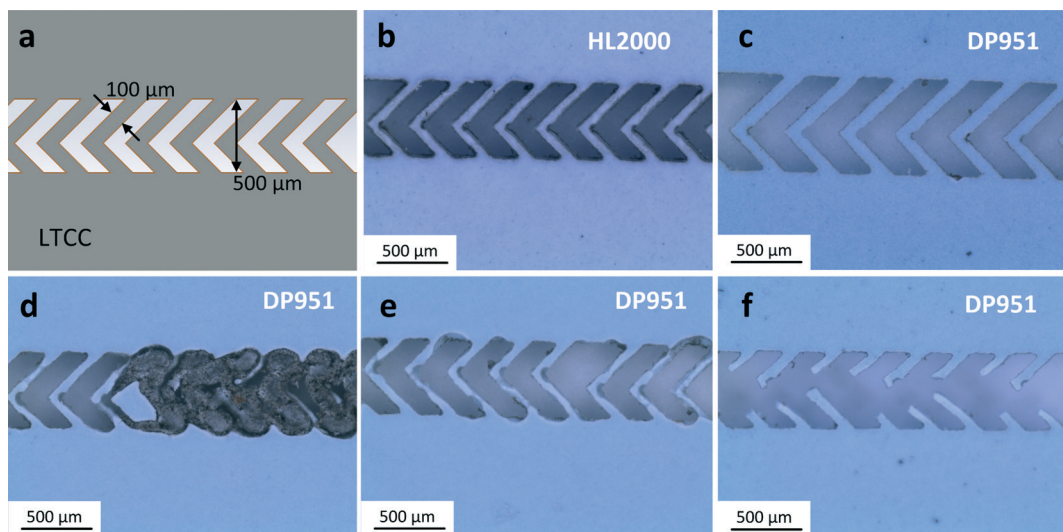


Fig. 4 (a) Schematic views of the herringbone fluidic structure layout; (b) HL2K and (c) DP951 with laser-machined herringbone structures using the optimized laser process. Optical images of the structure failures in the DP951 tapes due to inadequate laser process parameters: (d) incomplete laser cuts, (e) side wall bulging and (f) damaged herringbone structures.

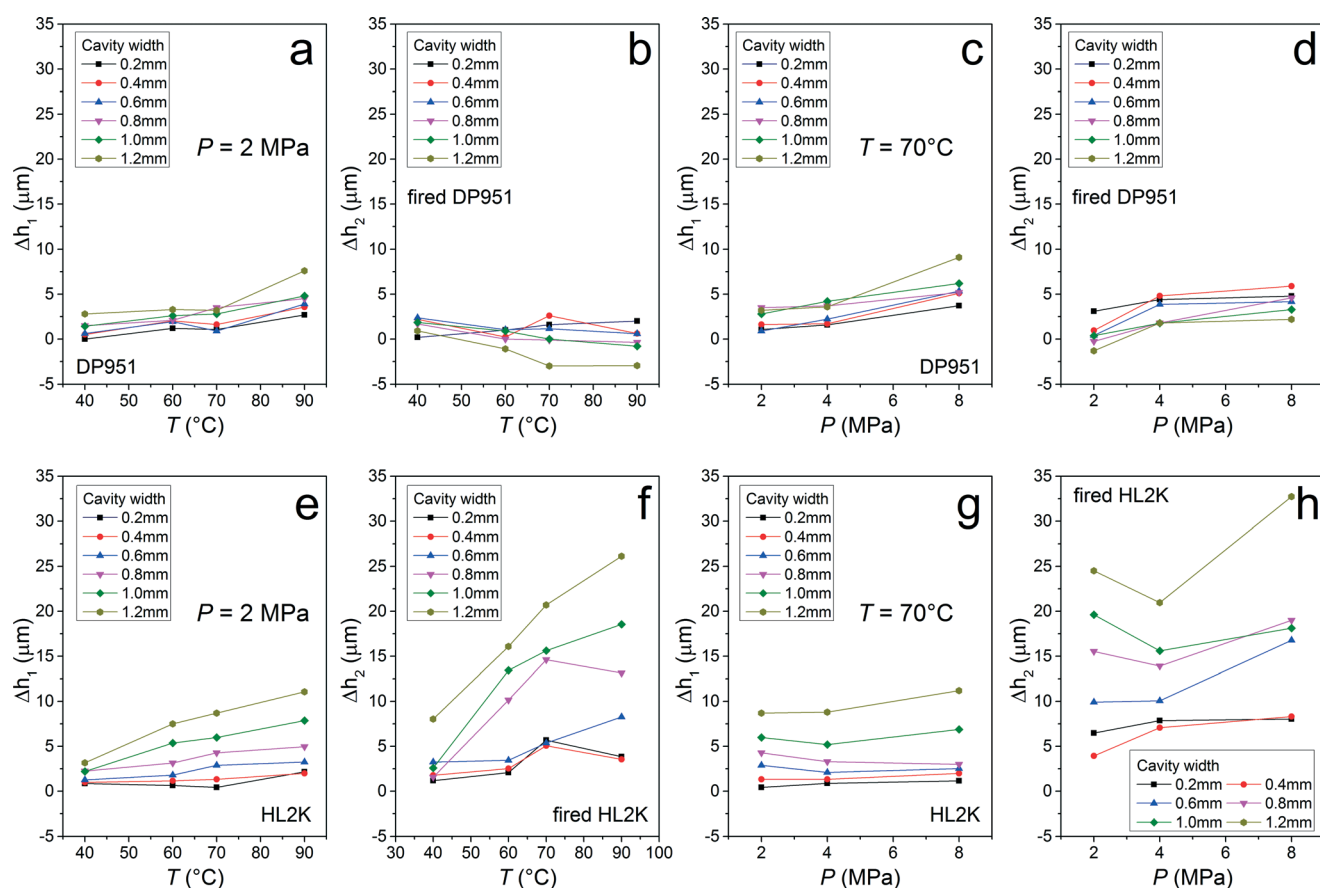


Fig. 5 Deflection results of the tested DP951 fluidic structure: samples (a) after lamination and (b) fired at various lamination temperatures; samples (c) after lamination and (d) fired at various lamination pressures. Deflection results of the tested HL2K fluidic structure: samples (e) after lamination and (f) fired at various lamination temperatures; samples (g) after lamination and (h) fired at various lamination pressures.

in the ESI†). With increasing T , as shown in Fig. 5a & e, the deflection change in HL2K was more dramatic than that in the DP951 ones. This may indicate that the HL2K samples

contained organic binders with lower glass transition temperature than these in the DP951 ones, resulting in more deformation.⁴¹ As T increased, these organic binders in the

stacked LTCC green tapes became less viscous, interpenetrated into the tapes at their interface, and promoted good joining of the laminates. However, this made the tapes mechanically weak, especially the cavity walls with mechanical supports that are sensitive to externally applied forces and easily become deformed, leading to sagging or even collapse. High T , P and W were found to promote these deformations. Hence, the lamination conditions, geometry of embedded cavities, thickness of cavity walls and types of used LTCC materials must be considered carefully in order to achieve good quality of embedded fluidic structures.

The LTCC firing process is also critical to the quality of these embedded cavities, as the capillary force of the melted glass phase in the laminates and their physical shrinkage in the planar direction can deform or even destroy the embedded fluidic structure.^{23,42} Both the DP951 and HL2K samples, laminated under varying T and P , were sintered under their standard firing profiles (see Table 2). Interestingly, the results showed very different deformation profiles for the two kinds of LTCC materials (see Fig. 5b, d, f & h). In the case of DP951, the deformation appeared to be reduced largely after firing. A negative value of deflection was even found for cavities with $w \geq 0.6$ mm and $T \geq 70$ °C (see Fig. 5b), indicating that a concave deformation changed to a swelling shaped deformation. Upon firing, the organic binders burnt out of the laminates and the contained glass phase melted, dissolving ceramic particles. As the pores in the laminate were filled by viscous flow of glass, the resulting densification led to large shrinkage in the planar direction. This suggests that the driving force of the shrinkage stretched the concave cavity walls, formed by lamination, against their own gravity during the densification process. Such a stretch, the so-called “drumhead” effect,⁴³ recovered the embedded cavities from their concave deformation and even resulted in a slight outward bulging. We speculate that this deformation recovery may result in increased local stress distribution at the edge of the suspending parts; however, no crack in this region was observed in all samples.

The results of the HL2K samples showed a different trend from that of the DP951 ones, in that the deformation of the cavity walls developed further (see Fig. 5f & h) after firing under all tested conditions, which is different from observations in previous studies.²³ For example, the deflection of the embedded cavities with $w = 1.2$ mm was almost 5 times more than those measured after lamination at either $T = 90$ °C and $P = 2$ MPa or $T = 70$ °C and $P = 8$ MPa as shown in Fig. 5f & h. Overall, we suggest that the deformation of the embedded cavities in HL2K is promoted by the firing process because its outer layers and refractory layer mutually constrain.

A straightforward way to improve the deformation is to increase the thickness of the embedded cavity walls or, in other words, enhance the mechanical strength of the suspended part over the embedded cavities in the laminate. The deflection of cavities in fired HL2K becomes less with the increasing thickness of the cavity walls (see Fig. S2†). For example, for the cavity with a width of 1.2 mm, the

deflection of the cavity wall was ~15 µm, much smaller than the one with the cover that has a green state thickness of 133 µm, produced under the same process conditions. This work also extended to the use of three HL2K green tapes as the cover layer, in which no noticeable deformation of embedded cavities was found. However, this approach may become constrained by the raw material cost, the device dimensions or some situations that require a thin cover layer, e.g. thermographic characterization.²¹

Based on these results, we found that the standard firing processes for both cases were still applicable in such a lamination method. The optimized low-pressure lamination conditions, for both DP951 and HL2K, in the multi-step lamination process can be summarized as $T = 60\text{--}70$ °C and $P = 2$ MPa, which result in minimal deformation of the embedded cavities. Besides, we would not recommend $T = 40$ °C for the fabrication of both DP951 and HL2K, as small delamination was found in some of the fired DP951 or HL2K samples (see Fig. 6a & b). Fig. 6c & d show the cross section of the tested samples with embedded cavities that were fabricated using the optimized processing parameters. No noticeable deformation of the cavity walls was observed for the DP951 or HL2K cases, even within embedded channels more than 3 mm wide. Particularly, DP951 shows much less deformation of the fabricated embedded cavities due to the “drumhead” effect.

Aside from deformation, the bonding of LTCC tapes is another important measure of the quality of microreactor fabrication. In the green state, such joining of the LTCC laminates is mainly dependent on the contained organic binders as well as mechanical bonding.¹³ As stated previously, both lamination pressure and temperature enhance the organic binders' fluidity, improving tape joining. Especially, the

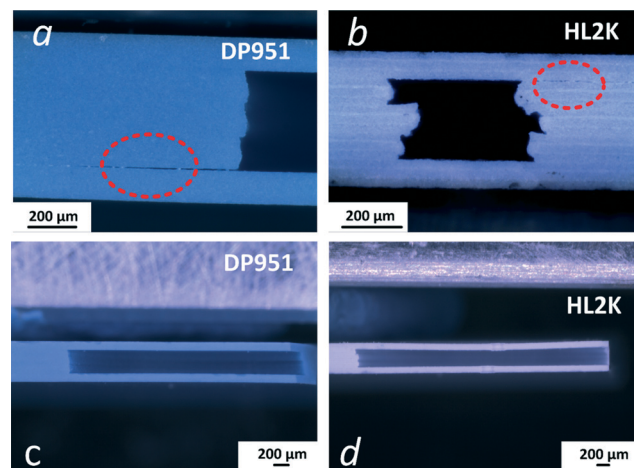


Fig. 6 Optical images of the cross section of fired LTCC with embedded cavities: delamination shown by red dashed lines for (a) DP951 and (b) HL2K samples at $T = 40$ °C and $P = 2$ MPa; halves of 5.0 mm wide cavities are shown in (c) DP951 and (d) HL2K using the optimized low-pressure lamination process ($T = 70$ °C, $P = 2$ MPa).

lamination pressure must be higher than the yield point of the organic binders to achieve good lamination. However, people have to be aware that too high lamination pressure would damage the embedded fluidic structure. Thus, a trade-off between the lamination process and the good quality of LTCC tape joining must be found. Here, due to difficulties in fabricating cross sections, we were unable to study the joining of LTCC samples in the green state, which might indicate that the unfired bonding strength is low. Another bonding mechanism occurs at the firing stage: the organic contents burn out and the glass melts to form viscous flow and bonds ceramics together as monolithic pieces.^{13,23} We did succeed in obtaining a cross section of these LTCC samples that were laminated using optimized process values and fired under standard conditions; no delamination or large pore formation was observed (see Fig. S3†). As compared to the DP951 samples that exhibit more monolithic bonding, the HL2K ones showed a kind of layered structure that was mainly due to the tape's sandwiched structure.³¹ It has been evidenced by Jurkow²³ that high porosity is obtained in such a layered structure of fired HL2K samples. This might result from HL2K's self-constrained sintering behavior and/or the incomplete burn out of organics. Nevertheless, using our developed process, embedded fluidic structures can be obtained with good quality of bonding and very limited deformation. It is very feasible to develop microreactors that usually have fluidic channels on the sub-mm scale using this process.

Applications

Disk-shaped passive micromixers

A LTCC-based disk-shaped micro-scale passive mixer has been developed successfully for the first time using our developed LTCC microfabrication process. This micromixer was designed as a single-channel continuous microreactor with a "T" type mixing entrance. In a fluidic channel, there is a series of tangential mixing channels with a disk shape, which has recirculation zones on each side of the structure with a major throughput at the center. Such a mixing design could effectively enhance the convective backmixing of reactant fluids and was reported in several stainless steel-based

microreactors for pharmaceutical productions.⁴⁴ Comparing with alloy-based microreactors, the LTCC ones have lower thermal conductivity, which would be greatly beneficial for studying the fluidic mixing of exothermic reactions as the thermal influence of the reactor bodies is very minimal. Using our developed laser cutting and multi-step lamination processes, LTCC micromixers, made of DP951 LTCC tapes, were successfully developed with an embedded disk-shaped mixing fluidic structure. In the 30 mm long mixing channel, there were 8 disk-shaped mixing structures with a diameter of 2.0 mm, as shown in Fig. 7a. The top wall of the fluidic channel after firing was only 100 µm thin (not shown). The profilometric results of this cover indicated deformation with a concave shape that is 20 µm deep at most for the embedded disk-shaped cavities, as compared with the 500 µm high deformation in the fluidic channels (see Fig. 7b). The dimensional deviation of the top cavity wall from the fluidic channels is only about 4%. A mixture of sulfuric acid (7.5 mol L⁻¹) and pseudoionone (1.2 mol L⁻¹) was used as a model reaction to examine the device's performance on the basis of its quasi-instantaneous exothermic characteristics.²¹

Continuous monitoring of a chemical reaction inside such small channels is generally challenging. Typically, the approach to use in our studies is rather qualitative, *i.e.* characterize the reaction kinetics and thermodynamics, which in turn allows the design of a stable chemical process. In such cases, it is enough to monitor the conditions at the inlet and outlet of the reactors. In addition, with the help of the thin top cover layer, an infrared thermographic method was able to visualize temperature profiles along the mixing channel. The results showed that the temperature reached its maximum at the middle of the mixing channel (see Fig. 7c), suggesting that good mixing occurred there at a 0.47 m s⁻¹ flow rate of feedstock ($Re \approx 75$).⁴⁵ This application proves our LTCC micro-fabrication process as a fast, inexpensive and flexible method for developing liquid phase continuous flow channel reactors.

Staggered herringbone micromixers

Recently, a chaotic mixing layout, the so-called staggered herringbone structure, has been proposed for efficient

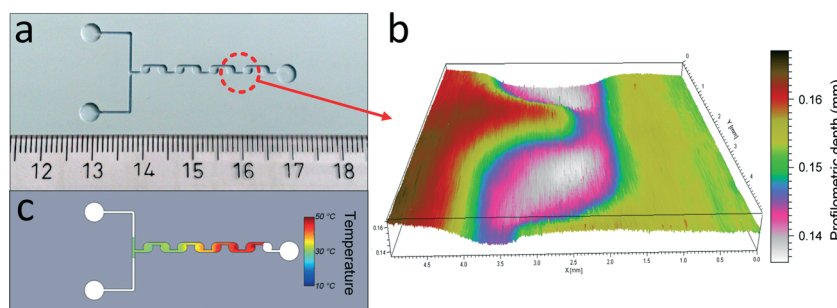


Fig. 7 A disk-shaped LTCC micromixer for chemical mixing applications: (a) top-view of the LTCC micromixer without a top cover; (b) profilometric results of the LTCC micromixer with a top cover (thickness ≈ 100 µm); (c) infrared results of the disk shaped microchannel mixing of sulfuric acid (7.5 mol L⁻¹) and pseudoionone (1.2 mol L⁻¹) at a high flow rate (0.47 m s⁻¹).

mixing at very low Reynolds numbers ($Re < 100$) in continuous-flow microchannel reactors.⁴⁶ Such a mixer contains a series of grooves built on the bottom side of fluidic channels. By altering the directions of such grooves, the structure can enforce flows to be folded successively on top of each other and thus produce effective chaotic advection for mixing of the fluids. We have exclusively reported LTCC-based microreactors with integrated staggered herringbone structures for fluidic mixing applications. The optimized laser micromachining and multi-step lamination processes allowed the production of 96 μm wide grooves at the bottom channel walls in the microreactors (see Fig. 8a). Using the same model reaction as described above, the thermographic results demonstrated that effective mixing occurred 18 mm away from the mixing point in a 30 mm long fluidic channel (see Fig. 8b) at $Re = 20$ of feedstock (flow rate 0.12 m s^{-1}). Comparing with ones without staggered herringbone structures, the mixing performance was greatly improved in these LTCC microreactors at such a low feeding rate.²¹

Multiple-injection microreactors for ionone production

The liquid-phase cyclization of pseudoionone is an important chemical process for producing α - and β -ionones that are extensively used in the pharmaceutical and fragrance industries.⁴⁷ However such a process takes place only in the presence of sulfuric acid. This is a quasi-instantaneous exothermic reaction. Due to the very fast kinetics, mixing of sulfuric acid and pseudoionone plays a crucial role since the acid concentrations influence product distribution and the global transformation rate. Undesirable hot spots can be easily formed in the microreactor, leading to low yields of ionones and their polymerization. The latter one in turn can produce more exothermic reactions and results in the clogging of fluidic channels.⁴⁸ Even by using microreactors with materials of high thermal conductivity, the overshooting temperature at the mixing point cannot be avoided. Therefore, the concepts of multiple-injection and heat exchangers

were proposed for better temperature control in continuous-flow microreactors for ionone production.²¹ Fig. 9a depicts the design of our developed LTCC multiple-injection microreactor. The device consists of two fluidic parts, with 7 functional layers: (a) the upper reaction part has three injection inlets and corresponding fluidic channels, each of which contains a series of staggered herringbone mixing channels and an interconnection channel; (b) the bottom part encloses three individual cooling channels (8.8 mm in width) running isopropanol coolants beneath the reaction channels.

The temperature profile of the chemical reaction was experimentally visualized by infrared thermography. Using the single injection method, the temperature rose significantly more than 25% of the adiabatic temperature in the herringbone mixing channel (see Fig. 9b). In contrast, the temperature raise was only 12% of the adiabatic temperature using the multiple-injection method with three injection points. Moreover, the temperature in the interconnection channels was cooled more efficiently by the integrated heat-exchangers due to the large heat exchanging area of the channel wall (see Fig. 9b). The overall reaction temperature was well-controlled in the range of 30–60 °C with the help of the gradual mixing of the reactants along the herringbone mixer and the active cooling. Consequently, a combined yield of α -ionone and β -ionone of over 98% was achieved in the device, using a total flow rate of 0.18 m s^{-1} of 7.5 mol L^{-1} sulfuric acid and 1.5 mol L^{-1} pseudoionone. This development proves the extensive capability of the LTCC microfabrication process for developing complex meso-scale microreactors, which are able to incorporate various functional fluidic structures together as one monolithic piece, for performing chemically harsh and exothermic reactions, especially those that are not dependent on the intrinsic kinetics but are controlled by the mixing of chemical reactants.

Further applications of such LTCC-based microreactors may be found in the laboratory as well as in large-scale chemical production. In the former case, this kind of microreactor can be used to generate understanding of a specific

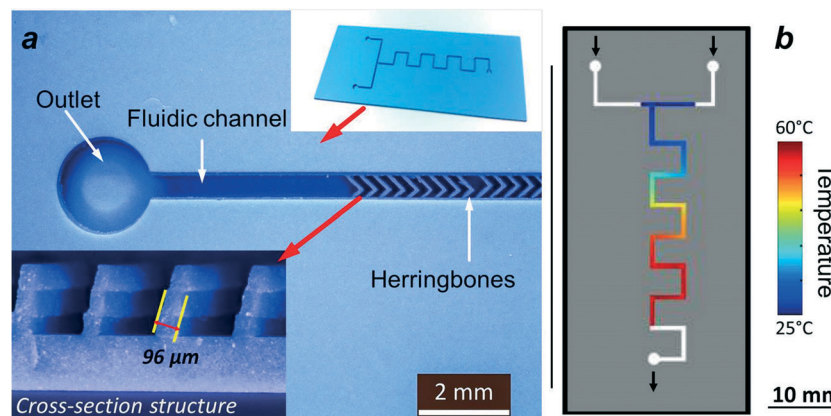


Fig. 8 An LTCC microreactor (without a top cover) with herringbone structures for chemical mixing applications: (a) microstructural images of a fabricated microreactor containing a staggered herringbone structure in a fluidic channel; (b) infrared results of the microreactor channel mixing of sulfuric acid (7.5 mol L^{-1}) and pseudoionone (1.2 mol L^{-1}) at a low flow rate (0.12 m s^{-1}).

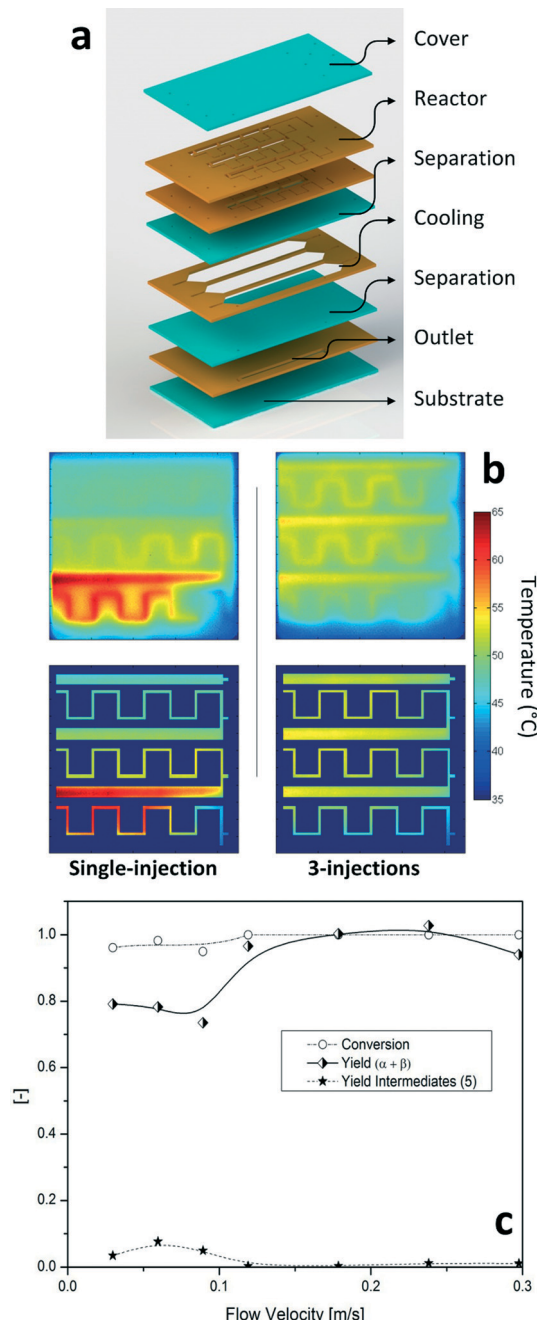


Fig. 9 A multiple-injection LTCC microreactor with integrated herringbone mixers and a cooling function for ionone production: (a) a schematic view of the multiple-injection LTCC microreactor; (b) thermographic results of the microreactor running in the single-injection and 3-injection modes; and (c) chemical analysis at various flow rates using the 3-injection operation.

reaction (kinetics and thermodynamics). Especially, monitoring tools can be integrated directly into the microreactor channels, for instance, temperature and pressure sensing probes, which opens a wide field of opportunities for this type of device. More specifically, one can use the hydrophilic wall properties (see Fig. S4†) to create droplets of organic compounds in an aqueous phase, allowing precise kinetic

models of any organic reaction to be established in a similar fashion as described by Kashid *et al.*⁴⁸ The use of the LTCC microreactor in production is rather limited to quasi-instantaneous reactions, as the maximum volume provided with this kind of microreactor is in the range of milliliters. The most prominent examples for this case are organometallic reactions such as those involving Grignard reagents.

High-temperature microreactors for hydrogen production

Another good example of LTCC microreactor made by our developed LTCC microfabrication process is the portable high-temperature (>400 °C) LTCC hydrogen generator.²⁰ In this work, the catalytic partial oxidation of propane for producing hydrogen was used as the model reaction. Ru-containing nanoparticles on inert ceramic supports were applied as catalysts (see Fig. 10c).

As shown in (see Fig. 10a), the microreactor has a slender bridge design and contains two working zones: (i) a hot zone for the chemical reaction and (ii) a cold zone, where standard fluidic and electrical interconnections can be used without concerns of thermal stability. The integrated thick-film heaters (see Fig. 10b) enabled to heat up the hot zone above 600 °C, while the bridge structure provided effective thermal decoupling for the cold zone to remain under 80 °C. Several fluidic structures with varying functionalities were able to be integrated in the hot zone: (a) gas distributors were placed at the entrance of the packed bed for better distribution of inflows (see Fig. 10d); (b) a packed-bed chamber having dimensions of $19.7 \times 12.0 \times 2.0$ mm³, with a catalyst loading window, for performing the catalytic partial oxidation (see Fig. 10e); (c) a middle layer with embedded thick-film heaters separated the packed bed and exit chambers and provided thermal energy to the reaction locally, in which the heaters also functioned as temperature sensors for monitoring the chemical process (see Fig. 10b); and (d) an exit outlet chamber below the middle layer connected the packed bed to the cold zone (see Fig. 10e). Using our developed micro-fabrication strategy, microreactors with these fluidic structures were able to be fabricated with very minimal deformation, especially the gas distributors with multiple micron-sized honeycomb channels and large suspended reactor walls over the reaction chamber (see Fig. 10b, d & e). Using such a bridge structure design (see Fig. 10a), the LTCC microreactor enabled to achieve two working zones in one device at different temperatures. The infrared thermographic result (see Fig. 10f) indicates that the “hot” area for chemical reactions reached an average temperature of 400 °C, heated by the embedded thick-film heaters, and the temperature of the “cold” area was kept below 100 °C, where standard electrical/fluidic interconnections can be used for integrating processing monitoring tools, *e.g.* temperature and pressure sensors. More information on such thermal design and characterization can be found in our previous work.²⁰

This device, fed with 0.01 m s^{-1} propane and air mixture, achieved a combined yield of hydrogen and carbon monoxide

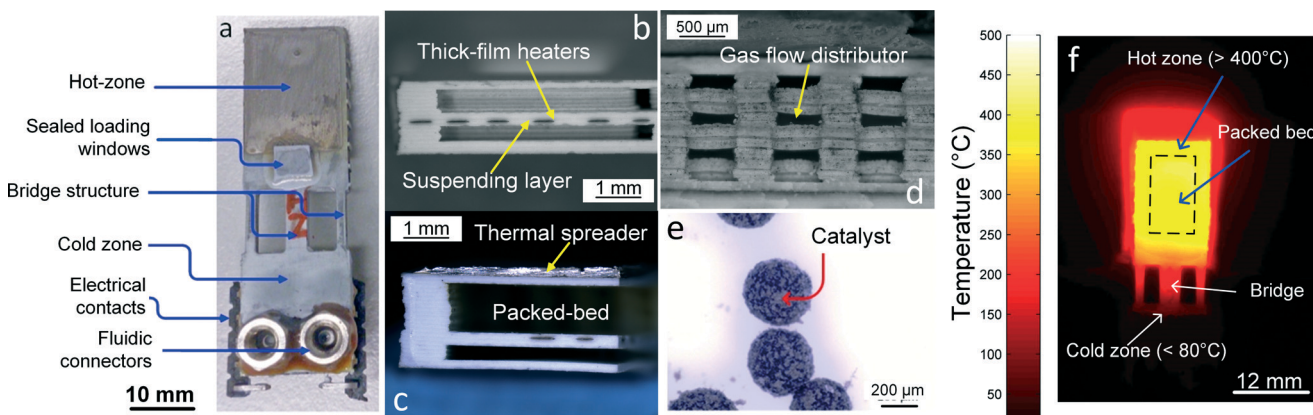


Fig. 10 An LTCC microreactor for high temperature ($>400\text{ }^{\circ}\text{C}$) hydrogen production via partial oxidation of propane: (a) a photo of the LTCC microreactor; (b), (d) and (c) structural images of fluidic channels at the cross section of the microreactor; (e) a photo of the used catalyst; and (f) an infrared image of the LTCC microreactor operating at an average temperature of $400\text{ }^{\circ}\text{C}$.

up to 71% at a reactor operating temperature of $642\text{ }^{\circ}\text{C}$. The overall reaction lasted for more than 5 hours, and no structural or electronic failure was observed in the devices, showing the high resistance of LTCC microreactors to high temperature ($>400\text{ }^{\circ}\text{C}$) environments. More importantly, the development of microreactors not only proves the versatility of LTCC fluidic fabrication for constructing complex fluidic channels, but also demonstrates multi-functionalities with integrated heating and temperature sensing abilities, which could be very beneficial to accurate process control and automation.

Conclusions

A novel low-temperature co-fired ceramic microfabrication process was developed to integrate various intact and complex fluidic channels into microreactors enabling them to perform chemical reactions under harsh conditions. Especially, the material stability test shows the high chemical resistance of fired LTCC to concentrated basic and acid solutions.

The fabrication method consists of optimized laser micromachining, multi-step lamination and a standard firing step. Our study showed that both laser processing parameters and LTCC green tapes have strong influence on structuring fine fluidic features. Staggered herringbone structures, on a scale of $100\text{ }\mu\text{m}$, were for the first time fabricated successfully in the LTCC green tapes. For the multi-step lamination, our profilometric results and cross section examination showed that mm-scale fluidic channels were able to be integrated into meso-scale microreactors without any sagging or collapsing. Limited deformation was only found in those cases involved with thin fluidic walls ($<120\text{ }\mu\text{m}$) or large suspending layers ($\sim 230\text{ }\mu\text{m}^2$). More importantly, this process does not require any additional chemical assistance or sacrificial volume materials and is feasible for the use of standard manufacturing firing process.

Various microreactors based on our developed LTCC fabrication strategy were demonstrated exclusively in applications of high-temperature and chemically harsh reactions.

1) A passive disk-shaped tangential micromixer was developed with a thin top fluidic wall ($\sim 100\text{ }\mu\text{m}$) for thermographic characterization of exothermic mixing reactions.

2) A micromixer with an incorporated staggered herringbone mixing structure was achieved which delivered efficient mixing of 7.5 mol L^{-1} sulfuric acid and 1.2 mol L^{-1} pseudoionone at low Reynolds number of feedstock ($\text{Re} \approx 20$).

3) A multi-injection microreactor was demonstrated for ionone production, in which the staggered herringbone mixing structure, the multiple injection fluidic channels and the liquid phase heat exchangers were incorporated successfully. The device led to a combined yield of α -ionone and β -ionone over 98% from the cyclization of pseudoionone at a total flow rate of 0.18 m s^{-1} .

4) A high temperature microreactor for portable hydrogen production was developed with integrated thick-film heating elements and a catalytic packed bed. The device was able to be self-heated up over $600\text{ }^{\circ}\text{C}$ in specific areas, while the other parts remained at low temperature ($<100\text{ }^{\circ}\text{C}$) where standard fluidic and electrical connections can be used. The microreactor delivered a combined yield of hydrogen and carbon monoxide as high as 71% from 0.01 m s^{-1} feed of air and propane mixture at $642\text{ }^{\circ}\text{C}$.

Our advancements largely reduce the development cycle of microreactors and simplify their fabrication process, especially in comparison with silicon-based microfabrication techniques. It provides a promising solution for simple, cheap and fast manufacturing of ceramic-based microreactor systems.

Acknowledgements

The authors would like to thank the Swiss National Science Foundation (contract number: 200021_143424/1) and the 7th European Framework Programme COPIRIDE project (contract number: CP-IP 228853-2) for financial support. The authors also appreciate Dr. Lovro Gorjan for his discussion and suggestions.

References

- 1 B. Ahmed-Omer, J. C. Brandt and T. Wirth, *Org. Biomol. Chem.*, 2007, **5**, 733–740.
- 2 T. Wirth, *Microreactors in Organic Chemistry and Catalysis*, Wiley. com, 2013.
- 3 R. Knitter, D. Göhring, P. Risthaus and J. Haußelt, *Microsyst. Technol.*, 2001, **7**, 85–90.
- 4 J. Vican, B. F. Gajdeczko and F. L. Dryer, *Proc. Combust. Inst.*, 2002, **29**, 909–916.
- 5 F. Meschke, G. Riebler, V. Hessel, J. Schürer and T. Baier, *Chem. Eng. Technol.*, 2005, **28**, 465–473.
- 6 Christian, M. Mitchell, D. P. Kim and P. J. A. Kenis, *J. Catal.*, 2006, **241**, 235–242.
- 7 T. Okamasa, G.-G. Lee, Y. Suzuki, N. Kasagi and S. Matsuda, *J. Micromech. Microeng.*, 2006, **16**, S198–S205.
- 8 M. Hrovat, D. Belavicić, G. Dolanc, P. Fajdiga, M. Santo-Zarnik, J. Holc, M. Jerlah, K. Makarović, S. Hocevar and I. Stegel, *Informacije MIDEM - Journal of Microelectronics, Electronic Components and Materials*, 2011, **41**, 171–178.
- 9 D. Belavić, M. Hrovat, G. Dolanc, M. Santo Zarnik, J. Holc and K. Makarović, *Radioengineering*, 2012, **21**, 195–200.
- 10 C. S. Martínez-Cisneros, S. Gómez-de Pedro, M. Puyol, J. García-García and J. Alonso-Chamarro, *Chem. Eng. J.*, 2012, **211–212**, 432–441.
- 11 C. Jacq, T. Maeder and P. Ryser, *Sadhana*, 2009, **34**, 677–687.
- 12 C. Bienert and A. Roosen, *J. Eur. Ceram. Soc.*, 2010, **30**, 369–374.
- 13 Y. Imanaka, *Multilayered low-temperature co-fired ceramics (LTCC) technology*, Springer US, Boston USA, 2004.
- 14 N. Ibáñez-García, J. Alonso, C. S. Martínez-Cisneros and F. Valdés, *TrAC, Trends Anal. Chem.*, 2008, **27**, 24–33.
- 15 C. Atzlesberger and W. Smetana, presented in part at the *30th International Spring Seminar on Electronics Technology*, Cluj-Napoca, Romania, 2007.
- 16 K. Schindler and A. Roosen, *J. Eur. Ceram. Soc.*, 2009, **29**, 899–904.
- 17 S. P. Wilhelm, R. W. Kay, M. I. Mohammed, Y. Lacotte and M. P. Y. Desmulliez, *Microsyst. Technol.*, 2013, **19**, 801–807.
- 18 W. Smetana, B. Balluch, G. Stangl, S. Lüftl and S. Seidler, *Microelectron. Reliab.*, 2009, **49**, 592–599.
- 19 K. Malecha, D. Jurkow and L. J. Golonka, *J. Micromech. Microeng.*, 2009, **19**, 065022–065022.
- 20 B. Jiang, T. Maeder, A. J. Santis-Alvarez, D. Poulikakos and P. Muralt, *J. Power Sources*, 2015, **273**, 1202–1217.
- 21 J. Haber, B. Jiang, T. Maeder, A. Renken and L. Kiwi-Minsker, *Green Processes Synth.*, 2013, **2**, 435–449.
- 22 K. Malecha, L. J. Golonka, J. Bałdyga, M. Jasińska and P. Sobieszuk, *Sens. Actuators, B*, 2009, **143**, 400–413.
- 23 D. Jurkow and L. Golonka, *J. Eur. Ceram. Soc.*, 2012, **32**, 2431–2441.
- 24 A. Roosen, *J. Eur. Ceram. Soc.*, 2001, **21**, 1993–1996.
- 25 D. Jurkow and L. Golonka, *Int. J. Appl. Ceram. Technol.*, 2010, **7**, 814–820.
- 26 J. A. Lewis, *Annu. Rev. Mater. Sci.*, 1997, **27**, 147–173.
- 27 H. Birol, T. Maeder, C. Jacq, S. Straessler and P. Ryser, *Int. J. Appl. Ceram. Technol.*, 2005, **2**, 364–373.
- 28 K. Malecha, T. Maeder and C. Jacq, *J. Eur. Ceram. Soc.*, 2012, **32**, 3277–3286.
- 29 E. Horváth and G. Harsányi, *Periodica Polytechnica Electrical Engineering and Computer Science*, 2010, **54**, 79–79.
- 30 W. K. Jones, Y. Liu, B. Larsen, P. Wang and M. Zampino, *Int. J. Microcircuits Electron. Packag.*, 2000, **23**, 469–473.
- 31 T. Rabe, W. A. Schiller, T. Hochheimer, C. Modes and A. Kipka, *Int. J. Appl. Ceram. Technol.*, 2005, **2**, 374–382.
- 32 DuPont 951 LTCC Green TapeTM, E.I. DuPont de Nemours and Company, 2001.
- 33 HERALOCKTM HL2000 Materials System, Heraeus, Circuit Materials Division, 2012, pp. 1–14.
- 34 K. M. Nowak, H. J. Baker and D. R. Hall, *Appl. Phys. A: Mater. Sci. Process.*, 2010, **103**, 1033–1046.
- 35 J. Zhu and W. K. C. Yung, *Int. J. Adv. Manuf. Technol.*, 2009, **42**, 696–702.
- 36 M. F. Shafique, A. Laister, M. Clark, R. E. Miles and I. D. Robertson, *J. Eur. Ceram. Soc.*, 2011, **31**, 2199–2204.
- 37 W. Zhang and R. E. Eitel, *Int. J. Appl. Ceram. Technol.*, 2012, **9**, 60–66.
- 38 T. Maeder, C. Jacq, Y. Fournier, W. Hraiz and P. Ryser, presented in part at the *17th European Microelectronics & Packaging Conference (EMPC)*, Rimini, Italy, 2009.
- 39 M. Gemeinert, *Doktor-Ingenieur*, der Technischen Universität Bergakademie Freiberg, 2009.
- 40 J. Kita, A. Dziedzic, L. J. Golonka and T. Zawada, *Microelectron. Int.*, 2002, **19**, 14–18.
- 41 B. Balluch, S. Lüftl, S. Seidler and W. Smetana, presented in part at the *International Conference of IMAPS Poland Chapter*, Pultusk, Poland, 2008.
- 42 L. E. Khoong, Y. M. Tan and Y. C. Lam, *J. Eur. Ceram. Soc.*, 2009, **29**, 2737–2745.
- 43 Y. Fournier, T. Maeder, G. Boutinard-Rouelle, A. Barras, N. Craquelin and P. Ryser, *Sensors*, 2010, **10**, 11156–11173.
- 44 N. Kockmann, M. Gottspöner and D. M. Roberge, *Chem. Eng. J.*, 2011, **167**, 718–726.
- 45 J. Haber, B. Jiang, N. Borhani, T. Maeder, J. R. Thome, A. Renken and L. Kiwi, presented in part at the *9th European Congress of Chemical Engineering (ECCE)*, The Hague, Holland, 2013.
- 46 N.-T. Nguyen and Z. Wu, *J. Micromech. Microeng.*, 2005, **15**, R1–R16.
- 47 V. K. Díez, B. J. Marcos, C. R. Apesteguía and J. I. Di Cosimo, *Appl. Catal., A*, 2009, **358**, 95–102.
- 48 M. N. Kashid, I. Yuranov, P. Raspail, P. Prechtel, J. Membrez, A. Renken and L. Kiwi-Minsker, *Ind. Eng. Chem. Res.*, 2011, **50**, 7920–7926.